Projecting future crop productivity for global economic modeling

Christoph Müller and Richard D. Robertson

Abstract

Assessments of climate change impacts on agricultural markets and land-use patterns rely on quantification of climate change impacts on land productivity and its spatial patterns. We here supply a set of climate impact scenarios on agricultural land productivity which is derived from two climate models and two biophysical crop growth models to account for some of the uncertainty inherent in climate and impact models. Aggregation in space and time leads to information losses that can determine climate change impacts on agricultural markets and land-use patterns because often aggregation is across steep gradients from low to high impacts or from increases to decreases. The four climate change impact scenarios supplied here were designed to represent the upper end of impacts (high emission scenario only, assumed ineffectiveness of CO_2 fertilization on agricultural yields, no adjustments in management) but consistent with the assumption that changes in agricultural practices are covered in the economic models. Globally, production of individual crops decrease by 10 to 38% under these climate change scenarios, with large uncertainties in spatial patterns that are determined by both the uncertainty in climate projections and the choice of impact model. This uncertainty in climate impact on crop productivity needs to be considered by economic assessments of climate change.

1 Introduction

For the assessment of future climate change impacts on land-use patterns and agricultural markets, the AgMIP project (agmip.org) (Rosenzweig, et al., 2013b) together with the ISI-MIP project (isi-mip.org) has conducted multi-model simulations with harmonized data on future yield changes. These scenarios are designed to assess the upper end of climate change impacts, therefore addressing only a high-emission scenario, RCP8.5 (Moss, et al., 2010, Riahi, et al., 2011) and without considering possible growth-enhancing effects of higher atmospheric carbon dioxide concentrations ([CO_2]), which are subject to large uncertainties (Long, et al., 2006, Tubiello, et al., 2007) and require adjustments in management (Ainsworth and Long, 2005). The assessment of future climate change impacts on agricultural productivity is complex and the many interacting processes contribute to their large uncertainty (Müller, 2011, Müller, et al., 2011, Rötter, et al., 2011, Roudier, et al., 2011, Knox, et al., 2012). To account for the degree of uncertainty in climate projections (Randall, et al., 2007, Hawkins and Sutton, 2009, Hawkins and Sutton, 2011) and in yield projections (Rötter, et al., 2011), we supply yield projections from 2 global crop growth models, DSSAT (Jones, et al., 2003, Hoogenboom, et al., 2004) and LPJmL (Bondeau, et al., 2007, Fader, et al., 2010, Waha, et al., 2012, Schaphoff, et al., 2013) for 2 implementations of the RCP8.5 emission scenario in general circulation models (GCMs), HadGEM2-ES (Jones, et al., 2011) and IPSL-CM5A-LR (Dufresne, et al., 2013). These 2 crop models (DSSAT as a widely used field scale model and LPJmL as a widely used ecosystem based model) represent the two different groups of gridded global crop models. For more details on the differences between these model groups, see Rosenzweig et al. (2013a).

For global economic models, these biophysical climate change impacts on yields need to be aggregated and assigned to appropriate spatial and thematic entities, taking into account the variability of data requirements across the global economic models. This paper describes the simulation of changes in crop productivity under climate change and the aggregation of these simulation results for use in the ten global economic models that participate within this AgMIP project (Nelson, et al., 2013, von Lampe, et al., 2013) but also beyond.

2 Methods

2.1 Climate data

The high end emission scenario used here, the representative concentration pathway with a radiative forcing of 8.5 Wm^{-2} (RCP8.5) (Moss, et al., 2010) reaches atmospheric carbon dioxide concentrations ([CO_2]) of 540 ppm in 2050 and of 935 ppm in 2100. These emission scenarios have been implemented by various climate models (general circulation models, GCM, and earth system models, ESM) and have been supplied by the C5MIP project at http://cmip-pcmdi.llnl.gov/cmip5/ (Taylor, et al., 2012). Differences in the climate models lead to a spread in simulated temperature increase for a given greenhouse gas emission scenario (climate sensitivity) and in the variability (daily, monthly, seasonal) and spatial patterns of change in climate variables (Hawkins and Sutton, 2009, Hawkins and Sutton, 2011). Figures 1-4 show the change in temperature and precipitation patterns from the reference period (1980-2010) to the 2050s (2035-2065) for the HadGEM-ES2 (Jones, et al., 2011) and IPSL-CM5A-LR (Dufresne, et al., 2013) models as used here. These climate scenarios differ not only in the spatial patterns of climate change, but also in the seasonal distribution. At the level of food production units (FPU) (Cai and Rosegrant, 2002), seasonal temperatures can increase homogenously or heterogeneously, in which cases winter temperatures typically rise more strongly than summer temperatures. Differences in temperature increase by 2050 between seasons can be up to 5.4 °C and 2.6°C for HadGEM-ES2 and IPSL-CM5A-LR, respectively. Annual mean temperatures in the different FPUs are projected to increase by 1.45°C to 5.48°C (4.79°C) from 1990 (1981-2010) to 2050 (2035-2064), while changes in annual precipitation can range between increases of 49% (106%) and decreases of 29% (50%) in the HadGEM-ES2 (IPSL-CM5A-LR) scenario. A table with projected annual and seasonal climate change per FPU is supplied in the supporting online material.

<< Figure 1 about here >>

Climate scenarios were selected based on availability of bias-corrected data sets from the ISI-MIP project. Bias correction was conducted to correct for over- and underestimation of climate variables and their daily variability in each 0.5° * 0.5° pixel of the land surface (about 55.5km * 55.5km at the equator). The bias correction method builds on Piani et al. (2010) but preserves absolute temperature and relative precipitation changes. The WATCH data set, which provides a good representation of real meteorological events and climate trends (Weedon, et al., 2011) served as reference climate here. Monthly mean values were corrected with absolute (temperature) and relative (precipitation, radiation) offsets that correct for each month’s difference between the 40-year mean of the GCM-simulated historic period (1960-1999) and that of the observation-based values of the WATCH data. For daily minimum and maximum temperatures, also the mean distance between these 2 values is preserved in the historic period. Daily variance within a month was corrected to match observations in the historic period. More details on the bias correction procedure and the selection of climate and reference data can be found in the work of Hempel, et al. (2013).

Both crop growth models were driven by the climate data provided by ISI-MIP (daily data from 1951 to 2099) and a standard set of management data, in order to simulate current management systems.

LPJmL was driven with the daily ISI-MIP data on daily mean temperature (T), precipitation (PR), shortwave downward radiation (SW_{down}) and longwave net radiation (LW_{net}). As longwave net radiation was not supplied by ISI-MIP, we computed it from the supplied longwave downward radiation (LW_{down}) and computed longwave upward radiation (LW_{up}) from surface temperatures, which we assumed to be equal to daily mean temperatures (T) following the Stefan-Boltzmann-law (equation 1).

$$LW_{net} = LW_{up} - LW_{down} = \sigma T^4 - LW_{down} \quad (1)$$

Where σ is the Stefan-Boltzmann constant of 5.670373×10^{-8} W m^{-2} K^{-4}.

Daily weather information for DSSAT (Tmax, Tmin, PR, SW_{down}) was obtained in an indirect manner using a random weather generator (SIMMETEO) (Geng, et al., 1986, Geng, et al., 1988). The weather generator uses monthly and annual averages for climate variables (maximum and minimum temperatures, solar radiation, rainfall, and rainy days per month) to generate plausible daily realizations. The averages for each of these variables were obtained by taking the bias-corrected daily weather data from the GCMs (i.e., the data used for LPJmL) and aggregating over the appropriate years around the time intervals to be investigated (1981-2010 and 2035-2065). Random weather was generated for 80 growing seasons which resulted in 80 yields at each location modeled with the overall yield taken as the average over all 80 outcomes.

2.2 Computing climate change impacts on yields

For the simulations of climate change impacts in economic models, data on yield shifters is supplied for the entire global land surface (LPJmL) or current agricultural land (DSSAT) for all crops covered by the models for fully irrigated (i.e. no constraints on water supply) and rain-fed systems. To represent the assumed ineffectiveness of CO_2 fertilization at field scale, we here keep the atmospheric CO_2 concentrations constant at the baseline level which was separately set at 370ppm for LPJmL and 369ppm for DSSAT after the year 2000.

2.2.1 DSSAT

DSSAT is a framework for crop models that employs daily time-step weather information and keeps track of hydrology and nutrient cycles using a soil module which considers a variety of soil characteristics (Jones, et al., 2003, Hoogenboom, et al., 2004). We employed the CERES models for rice (*Oryza sativa*), wheat (*Triticum* spp.), and maize (*Zea mays*) and the CROPGRO models for soybeans (*Glycine max)* and groundnuts (*Arachis hypogaea*).

Soil. DSSAT's soil module employs a soil profile definition that details the various soil layers and their properties. The most salient of these characteristics are the soil depth, water parameters (lower limit, drained upper limit, and saturation), root growth factor, bulk density, organic carbon content, and texture fractions. Our approach employs generic soil profiles with typical values chosen for these quantities.

The twenty-seven generic profiles are a combination of three by three soil characteristics. The first defining characteristic is organic carbon content with high, medium, and low values. These are combined with deep, medium and shallow soil depth cases. Finally, there are three texture types: sandy, loamy, and clay-like. For each case, e.g., “high organic carbon deep loam” or “low carbon shallow sand”, a representative soil profile is available. Each location is assigned one of these representative soils based on thresholds and rules applied to the Harmonized World Soil Database (HWSD) (FAO/IIASA/ISRIC/ISSCAS/JRC, 2012). For more details on this parameterization of soil properties in DSSAT see (Koo and Dimes, 2010).

Initialization. Soil moisture in each soil layer is set to 25% of its water holding capacity at the beginning of the simulations (supplementary Figure S5). Stable carbon pools are set based on texture and depth (Basso, et al., 2011) (supplementary Figure S6-S7). Geographically distinct assumptions are made regarding root mass (supplementary Figure S8) and residues remaining from previous cropping activities (supplementary Figure S9) as well as initial soil nitrogen (supplementary Figure S10). Of these, the most influential is the initial soil nitrogen. After initialization, a spin-up period is employed. The simulation is begun 90 days prior to the anticipated planting date. The soil, hydrologic, and weather processes begin to operate and thus decrease the importance of the initial conditions.

Management. DSSAT yield simulations are not calibrated to yield statistics such as the FAO data base, but are determined by climate inputs and a set of management options, which is assumed to be static in time. The sowing dates are determined in four different ways, depending on the situation. We have developed rules which operate on monthly climate averages for temperatures and precipitation. These rules provide planting months for a generic rainfed crop (modeled on maize), a generic irrigated crop (modeled on rice; used when the rainfed rule fails), spring wheat, and winter wheat (Nelson, et al., 2010). This target planting month was determined using the climate averages from the 1981-2010 period and was used for both time periods. Adjusting planting dates was considered to be a form of adaptation that was to be captured in the economic models rather than at the biophysical stage. The actual planting date was determined by an automatic planting scheme in DSSAT. The planting window opens on the first day of the month determined by the rules. When the temperature and soil moisture fall within some predetermined bounds, the actual planting occurs, otherwise the repetition is excluded from the reported average over the 80 weather realizations.

Three major management considerations remain: fertilizers, irrigation, and harvesting. Nitrogen fertilizer application rate assumptions were made by geographic region (supplementary Figure S11-S13). The timing of fertilizer application was determined by rules based on the overall amount to be applied and the time to flowering and maturity. Each crop had specific rules. Irrigated conditions were intended to represent a minimal water stress situation (water availability and its effects were relegated to the domain of the economic models). An automatic irrigation scheme in DSSAT was used such that when the soil moisture of the upper 0.2 m falls below 70% of the water holding capacity, sufficient water is supplied to increase soil moisture to 100% of the water holding capacity. Harvest occurred at physiological maturity.

The CERES and CROPGRO models have the ability to represent a wide diversity in cultivars and thus particular choices had to be made concerning which varieties to use. The process was different for each crop, but usually involved several varieties along with maps indicating which geographic areas they were appropriate for. For rice a generic Japonica variety was used along with an Indica variety (supplementary Figure S14); for wheat eleven unique variety definitions were used; for maize two generic varieties were used corresponding to characteristics typical of developed world applications and the developing world; for groundnuts four varieties were used for the developing world and a single variety for the developed world; and for soybeans thirteen generic varieties were used (differentiated by maturity length) at each location, the highest yielding variety was chosen.

2.2.2 LPJmL

LPJmL is a global dynamic vegetation, hydrology and crop growth model (Bondeau, et al., 2007, Fader, et al., 2010, Waha, et al., 2012). It simulates crop yields of 12 different crops (Table 1), that represent the most important crop types globally (temperate and tropical cereals, maize, rice, pulses, temperate and tropical roots and tubers, soybeans, oilcrops) (Bondeau, et al., 2007) and sugarcane (*Saccharum* spp.) (Lapola, et al., 2009). The version used here employs the latest model improvements as a more complex soil hydrology as needed for the permafrost implementation (Schaphoff, et al., 2013) and an implementation of a linear LAI-FPAR model for maize (Zhou, et al., 2002) and the minimum root-to-shoot ratios at maturity were set to 10% (based on insights from the AgMIP wheat (Asseng, et al., 2013) and maize pilots & (Prince, et al., 2001)).

Soil. The improved soil representation of the model (Schaphoff, et al., 2013) covers the upper 3m of the soil in 5 layers. Rain, melt and irrigation water infiltrates at the surface and percolates to deeper layers if above field capacity. Soil temperatures are determined by a heat conductance energy model (Schaphoff, et al., 2013). Plants transpire water according to their root distribution over the soil layers (Jobbágy and Jackson, 2000), while soil water evaporates only from the upper 0.2m.

Soil data are taken from Harmonized world soil database (FAO/IIASA/ISRIC/ISSCAS/JRC, 2012). The classification is based on the USDA soil texture classification (http://edis.ifas.ufl.edu/ss169), the hydraulic soil parameters (saturated hydraulic conductivity [mm/h], water content at wilting point/field capacity/saturation) are derived from Cosby et al. (1984) and the thermal parameters (thermal diffusivity (mm^2/s) at wilting point, 15%, field capacity (100% whc), wilting point, saturation (all water), and saturation (all ice)) from Lawrence and Slater (2008), the suction head (mm) in Green-Ampt equation following Rawls, Brakensiek and Miller (1983).

Initialization. Soil conditions are not initialized but are determined in a 200-year spin-up simulation, recycling the first 30-years of that time series for the spin-up simulation. Such long spin-up is needed to ensure that soil temperatures are in equilibrium with climate before simulations start(Schaphoff, et al., 2013). Baseline and future conditions are simulated in a single transient run from 1951 to 2099, so that soil conditions in the future period (2050s) were determined by the simulated previous years.

Management. Apart from cultivar choices (Bondeau, et al., 2007), sowing dates (Waha, et al., 2012) and irrigation, management options are not treated explicitly in LPJmL. For the representation of current management patterns, national cropping intensity has been calibrated to FAO statistics as described in Fader et al. (2010). For this, three parameters, maximum leaf area index (LAImax m^2 of leaves per m^2 of ground), a scaling factor for scaling leaf-level photosynthesis to stand level (alphaA, Haxeltine and Prentice, 1996) and the harvest index (HI) are scaled in combination. LAImax can range from 1 (lowest intensity) to 7 (highest intensity), alphaA from 0.4 to 1 and HI has a CFT specific range (Bondeau, et al., 2007), which can be reduced by up to 20%, assuming more robust but less productive varieties in production systems with low productivity (Gosme, et al., 2010).

Accounting for the linear LAI-FPAR model for maize (Zhou, et al., 2002) and maximum intensity levels for maize now assume a maximum leaf area index of 5 instead of 7 as described by Fader et al. (2010). Nutrient dynamics are not explicitly represented in the model. Sowing dates have been computed as in Waha et al. (2012), but have been kept constant after 1951. The model decides internally whether to grow winter or spring wheat/rapeseed on wheat/rapeseed areas. It has a preference for winter varieties, but if winters are too long, it will grow spring varieties (Bondeau, et al., 2007). Algorithms to select varieties have been adjusted as described in Müller, et al. (2013). For irrigated crops, irrigation water is assumed to be available in unlimited supply. Irrigation is triggered if soil moisture falls below 90% of the water holding capacity. Harvest occurs at maturity.

2.3 Aggregation and extrapolation for economic models

Economic models that cover the agricultural sector work with very different resolutions of spatial, temporal and commodity resolutions, ranging from computable general equilibrium models (CGE, such as AIM (Fujimori, et al., 2012), EPPA (Paltsev, et al., 2005)), partial equilibrium models (PE, such as GCAM (Thomson, et al., 2011, Wise and Calvin, 2011), IMPACT (Nelson, et al., 2010, Rosegrant and IMPACT Development Team, 2012)) to land use models that combine economic rationale with spatially explicit biophysical data on crop yields and water availability (LUM, such as MAgPIE (Lotze-Campen, et al., 2008, Schmitz, et al., 2012) and GLOBIOM (Havlík, et al., 2011, Havlík, et al., 2013)). The representation of dynamics in agricultural land productivity and the production functions affected by this consequently differs among models and is not directly compatible with the characteristics of gridded global crop models. Consequently, climate change impacts on agricultural crop yields as computed by the agricultural biophysical impact models DSSAT and LPJmL have been aggregated and also extrapolated to match information requirements in economic models, which is described in detail below. For a detailed description of the economic models that participated in this AgMIP intercomparison see Nelson, et al. (2013) and von Lampe, et al. (2013).

2.3.1 Mapping of crops to commodities

The biophysical impact models DSSAT and LPJmL explicitly simulate a variety of crops; however, they do not match up precisely with the agricultural commodities represented in agricultural economic models. Simulated dynamics in crop productivity were used to determine dynamics in land productivity of the economic models' commodities, wherever possible. For those commodities which had no direct representation in the biophysical impact models, we used simulated climate change responses in similar crops to estimate their response to climate change. Similarity was based on the type of photosynthetic pathway (distinguishing C_3 crops from C_4 crops), their main climate zone (temperate vs. tropical) and their susceptibility to drought damage.

Following the crop-to-commodity mapping in Table 1, we supplied information on climate impacts on agricultural land productivity for 23 commodities. DSSAT simulations provide data on 5 different crops, wheat (whe), maize (mai), rice (ric), soybean (soy), and groundnut (grn). LPJmL simulations provide data for the 12 crops implemented in LPJmL, wheat, maize, rice, soybean, millet (*Pennisetum glaucum*, mill), rapeseed (*Brassica napus*, rap), sugar beet (*Beta vulgaris*, sugbe), sugar cane (sug), field peas (*Pisum sativum*, fpea), cassava (*Manihot esculenta*, cas), sunflower (*Helianthus annuus*, sunf), groundnuts, and managed grassland (gra). Both biophysical impact models supplied data separately for irrigated and rain-fed production.

2.3.2 Spatial resolution

While yield impacts have been computed on a regular geographic grid (30' resolution), most economic models require information for administrative units. Consequently, yield data have been provided at their original resolution and in aggregated form for the IMPACT food production units (FPUs)(Cai and Rosegrant, 2002), which could then be further aggregated to the individual economic models' needs. For the aggregation to FPUs, we used actual physical production areas for the individual crops from the SPAM data set, version 2 (You, et al., 2010). Combining the areas and yields allows us to calculate the regional area-weighted average yield for each case. Most crops simulated by LPJmL and DSSAT here could be aggregated using crop-specific land-use patterns from SPAM, however, sunflower and rapeseed yields were aggregated with the areas of *other oilcrops* in SPAM as no crop-specific area data are available for these crops.

Using production area information, rain-fed and irrigated crop production as simulated by the models could also be aggregated to overall crop productivity if the economic model does not distinguish rain-fed from irrigated production.

2.3.3 Temporal resolution

Due to the differences in handling the climate and weather data, the yields entering the climate change impact calculations are aggregated slightly differently for the two crop models. While LPJmL simulated agricultural productivity of crops in a transient run from 1951-2099, DSSAT simulated only the year 2000 and the year 2050, using 80 realizations of daily weather variations from its weather generator (Geng, et al., 1986, Geng, et al., 1988). We used the average of 2000 to 2009 to represent the LPJmL crop productivity in 2000 and the average of 2050 to 2059 for 2050.

To fill the years between 2010 and 2050 for DSSAT simulations, the climate change induced changes in agricultural productivity were supplied as annual growth rates (g) from simulated reference (p_{ref}) and future production (p_{fut}), following equation 2 so that climate change impacts can be computed for any year between 2010 and 2050 in the economic models.

$$g = (p_{fut} / p_{ref})^{1/40} - 1 \qquad (2)$$

For reasons of harmonization, data from LPJmL were also supplied in form of an annual growth rate. Additionally, due to the yearly yields available, annual and decadal effects were supplied. If an economic model is designed to take such information into account, this allows for addressing inter-annual/decadal variability of production,.

At the FPU-level, aggregated yield shifters have been capped to avoid being overly sensitive to variations and model artifacts that may occur if the biophysical crop models simulate very low reference period productivities. The upper limit for positive climate impacts on yields was set to an annual growth rate of 0.53%/year (equivalent to 23.5% increase in 40 years), negative impacts were limited to 2%/year (equivalent to 63% decrease in 40 years).

3 Results

In all scenarios analyzed here, climate change leads to strong decreases in agricultural productivity in most of the agricultural area, but with some notable exceptions such as currently temperature limited mountainous or high-latitude areas. At the global scale, crop yields decrease by 9.9 to 37.6% by 2050 for the five crops simulated by both models (Table 2). While there is high agreement at the global scale on climate change impacts on rice and groundnut productivity across the two crop models and the two climate scenarios, DSSAT projects substantially more detrimental impacts on maize (-35.8% vs. -12.1% respectively) and wheat (-19.4% vs. -12.2% respectively) than LPJmL. Generally, climate impacts on crop yields have similar distributions between the crop models and climate scenarios (Figure 2), but the spatial patterns of impact differ in some cases significantly (Figure 3-4 and supplementary Figures S15-S29). It is noteworthy that already moderate changes in crop productivity and crop production can have significant impacts on agricultural markets and prices. This was demonstrated in the recent drought in the USA in 2012, where maize yields and production decreased by 18% and 12% respectively, but US maize exports had almost dropped by 50% in October and November 2012 compared to the already low export quantities in 2011 and to about a third of the peak export quantities in 2007 (Capehart, et al., 2012).

<< Figure 2 about here >>

Figures 3-4 display spatial patterns for the crops as simulated by DSSAT and LPJmL for the 2 climate scenarios employed (also see supplementary figures for other crops). The spatial patterns of change cannot always be directly linked to the change patterns of climate variables and there are also differences between the 2 crop models' projections. While the impact patterns show many similarities between the models/scenarios, there are important differences. Rainfed wheat, for example is projected to increase in East (HadGEM and IPSL) and central (HadGEM only) Europe by DSSAT, while LPJmL simulates yield reductions throughout Europe. The slightly lower increases in annual mean temperature in HadGEM than in IPSL (Figures 1-2) lead to yield increases in the Russian-Kazakh border region in the HadGEM scenario but to decreases in the IPSL scenario. The main difference is that spring precipitation (March, April, May) is projected to increase significantly by HadGEM2-ES but to decrease in summer (June, July, August) while ISPL-CM5A-LR projects smaller variability of the seasonal distribution but rather sees a drying in spring and wetter conditions in summer in this region. Both agree on increasing winter precipitation (see supplementary Figure S1). For irrigated wheat productivity, DSSAT simulations are more optimistic in Europe and more pessimistic for India, China and Mexico (see also supplementary Figure S15).

<< Figure 3 about here >>

For maize, the spatial patterns of yield changes agree well between the two crop models, but DSSAT projects significantly stronger yield changes almost everywhere, including the yield increase in the high latitudes in both rainfed (Figure 4) and irrigated cultivation (supplementary Figure S16).

Groundnut simulations are similar between crop models but more severe for IPSL for rainfed and for DSSAT for irrigated cultivation (supplementary Figures S17-S18).

For rice productivity, climate impacts do not differ much between the two climate models but DSSAT is more pessimistic for irrigated rice, while LPJmL is more pessimistic for rainfed rice cultivation under climate change (supplementary Figures S19-S20).

For soy, there are significant regional differences between climate and crop model simulations for rainfed soy productivity, while DSSAT is often more optimistic for irrigated conditions (supplementary Figures S21-S22).

<< Figure 4 about here >>

Spatial variability of yields within food production units (FPUs) decreases more often than increases with climate change and more so in DSSAT simulations than in LPJmL (Fig 5) as does year-to-year variability both at the FPU (Fig 6) and grid cell level (supplementary figure S30) in LPJmL simulations.

<< Figure 5 about here >>

<< Figure 6 about here >>

A table with the crop-specific climate change impacts on yields per FPU for the four scenarios is supplied in the supporting online material.

4 Discussion

We here supply four scenarios of climate change impacts on crop yields, in high spatial and temporal resolution as well as in aggregated form in order to supply biophysical climate change impacts on crop productivity to economic models. The detail of information supplied, also in aggregated form allows for simulating changes in land use patterns, e.g. through land expansion, reallocation of cropping systems and land abandonment. Depending on mechanisms implemented in the economic models, costs for such changes in land-use patterns will have to be parameterized with observations (Schmitz, et al., 2013).

Given the low number of climate change impact scenarios (4), these can only partially cover the range of possible future climate change impacts. Even though these scenarios were designed to represent high-end climate change impact scenarios, not all assumptions and model implementations are on the pessimistic side. We use only scenarios of the highest emission scenario (RCP 8.5) of the most recent emission scenario set (Moss, et al., 2010), the crop models were set up to exclude any adaptation mechanism (such as the adjustment of sowing dates) and any possible positive effects of CO_2 fertilization were excluded here. However, several aspects are excluded that have the potential to further decline yields. Ozone damage can substantially reduce crop yields (Bender and Weigel, 2011, Leisner and Ainsworth, 2012) and ozone concentrations are projected to increase especially in Asia but are projected to decline in North America and stabilize in Europe under the RCP8.5 scenario (Wild, et al., 2012). While the model setup of DSSAT with synthetic daily weather data prevents a direct accounting for changes in weather extremes, LPJmL is driven with daily (bias-corrected) data from the GCMs. The model, however, does not cover mechanisms that would allow for an assessment of extreme events under climate change (no increased heat sensitivity at anthesis, no crop damage under intense precipitation events such as hail storms). The scenarios are thus assuming no effects of increasing extremes on crop productivity here, even though these can have significant effects on crop yields (Asseng, et al., 2011, Hawkins, et al., 2013). Indirect effects of climate change on crop growth through weeds, pests and pathogens are not covered by the crop growth models here.

The assumption of static management systems is not without caveats as there are also adaptation measures that potentially can be implemented with limited extra costs, such as the adjustment of sowing dates to climate change, which can strongly affect the strength of impacts (Laux, et al., 2010, Folberth, et al., 2012, Waha, et al., 2013). However this setting also helps to avoid overlapping assumptions in biophysical and economic models: All adaptation efforts to compensate negative climate change impacts are exclusively addressed in the economic models, while we here supply data on climate change impacts on agricultural productivity under static management assumptions only. Typically, adaptation in economic models is represented by a mixture of explicitly modeled mechanisms such as changes in resource allocation and/or in consumption patterns and aggregated response mechanisms, such as the investment in technological change, which does not distinguish individual measures such as breeding new varieties or better soil management (Dietrich, et al., 2012, Dietrich, et al., in press). For such aggregate adaptation mechanisms in economic models, adaptation options already included in the biophysical crop modeling cannot be excluded and the exclusion of adaptation measures in the crop models thus ensures consistency. This impedes a detailed analysis of adaptation options in agricultural production systems for which a stronger interaction between crop models and economic models would be necessary. The ability of the GLOBIOM model to select from different management systems per commodity (Havlík, et al., 2013) could facilitate an analysis of adaptation options in crop production management and via land-use change and price mechanism, but this detail in differences in sensitivity to climate change between crop management systems is not supplied here.

The effectiveness of CO_2 fertilization at field scale or even in national or global productivity and a crop model's ability to project it is subject to considerable uncertainty and scientific debate (Long, et al., 2006, Tubiello, et al., 2007). While assuming no CO_2 fertilization is clearly a pessimistic assumption here, it is consistent with the idea of leaving adjustments in management to the economic models: Any beneficial effect of CO_2 fertilization on crop yields will require an adjustment in management to enable higher quantities. Otherwise nitrogen could become limiting and could result in reductions in quality (e.g. protein content) (Leakey, et al., 2009, Bloom, et al., 2010, Parry and Hawkesford, 2010). Changes in the chemical composition of plants under elevated atmospheric CO_2 concentrations could also have detrimental effects on yields, as it was shown to impede the plants' defense mechanisms against insect damage (Dermody, et al., 2008, Zavala, et al., 2008) and may interfere with the enzyme and hormone regulation in plants (Ribeiro, et al., 2012). As both crop and economic models at the global scale are not capable address these detailed feedbacks and the assumption to ignore CO_2 fertilization effects is consistent with this.

The selection of global circulation models (GCMs) is based on availability of climate scenarios and the modeling protocol of ISI-MIP and AgMIP only; it does not reflect the range of uncertainties from different climate models.

The aggregation of spatially explicit simulations of crop yields under climate change to larger spatial units, as required for most economic models, is inconsistent with the simulated land-use change by these economic models. Only models that are able to process spatially explicit data are capable of responding to climate change impacts by reallocating production within spatial production units (FPUs, countries). This allows for more flexible response to climate change patterns, especially as the spatial variability of crop yields within FPUs (Fig 5) changes as well under climate change, which is independent of the direction of change.

The variability in time is estimated for LPJmL only, since DSSAT is driven with 80 replica of the same year. Results show that temporal variability of FPU production (expressed as the coefficient of variation over a 30-year period around 2000 and 2050) increases about twice as much (64%) than it decreases (29%, see Fig. 6), a ratio that is also observed at the pixel level (supplementary Figure S30) as well as for irrigated and rainfed systems individually (supplementary Figures S31-S32).

At the same time, models that use spatially explicit yield shifter data may also see different yield trends as their initial and changing land-use patterns will very likely lead to a different weighting scheme than used here based on the SPAM data. This means that climate change effects in economic assessments directly depend on the spatial aggregation method and can lead to different dynamics if aggregation weights (e.g. SPAM data vs. other land-use patterns) differ and if there are strong gradients in climate change within aggregation units. This is, e.g., the case in the USA (north-east for DSSAT, central for LPJmL) for wheat (Figure 3) or east China for maize (Figure 4). A direct comparison of economic models driven with spatially aggregated yield data and models driven with spatially explicit data is thus inhibited.

Mapping of simulated climate change impacts on specific crops to other crops and commodities not covered by the biophysical crop models is a suitable way to generate comprehensive climate change impact scenarios for all commodities. It is, however, also an additional source of uncertainty, especially if the plants' properties are not similar (e.g. fruits that are typically from dicotyledon and perennial plants vs. the average of rice, wheat (both monocotyledon), soybean and groundnut (both dicotyledon) which are annual plants, see Table 1).

Practical matters constrained how many and which crops were chosen for modeling. Of course, there are more crops cultivated than there are reliable models of them. Still, there are plenty of models; within the DSSAT framework, there are representations of potatoes, cassava, sugarcane, sorghum, millet, cotton, chickpeas, and more. The lack of reliable input information for these, as well as the additional computational and organizational burden of handling the results led to the focus on the five major crops of rice, wheat, maize, soybeans, and groundnuts.

The uncertainty associated with mapping simulated bio-physical climate change impacts on specific crops to economic commodities is illustrated well by the case of sugarcane. While we simulate sugarcane plants directly in LPJmL (Lapola, et al., 2009), we do not with DSSAT here, but assume that climate change impacts on sugarcane are identical to those on maize for

DSSAT-based yield shifters (Table 1). While this is a reasonable choice, as both maize and sugarcane are C_4 plants (while the other crops simulated with DSSAT are C_3 plants), there are some important differences between the 2 crops that limit the comparability. Most importantly, the economically valuable part of maize is the fruit of the plant, while it's the stalk in case of sugarcane. Climate change impacts are thus expected to be more severe in maize production, as the sensitive phenological stages of flowering and grain filling can be affected more strongly by climate change (Lobell, et al., 2011). Sugarcane productivity is also impacted by increasing temperatures, but radiation use efficiency (i.e. biomass accumulation per unit of light energy absorbed) only decrease at daily mean temperatures above 35°C (Singels, et al., 2005) and fruit development is unwanted, as flowering actually impinges on sugarcane yields (Berding and Hurney, 2005).

The two biophysical crop models employed here reflect the uncertainties in global crop modeling (Rosenzweig, et al., 2013a) to some extent. They differ with respect to model characteristics (e.g. radiation use efficiency model vs. more complex photosynthesis model) and management assumptions (cropping periods, co-limitation by nutrients vs. no explicit treatment of nutrients). Consequently, projections of climate change impacts on crop yields differ both at global (Table 2) and regional scales (Figures 3 and 4). While DSSAT simulations typically project stronger global impacts for wheat and maize than LPJmL, its projections of impacts for rice, soybean and groundnut are typically less detrimental than those of LPJmL. Differences between the climate scenarios are typically smaller than those between crop models at the global scale, but can be substantial in specific regions (e.g. rainfed maize in Europe for DSSAT or China for LPJmL, Figure 4).

Global-gridded approaches to crop modeling using climate change scenarios will help to illuminate these uncertainties in the economic realm leading to modeling improvements to reduce them as well as assessing and edifying the robustness of the biophysical models. Results from the global gridded crop model intercomparison of AgMIP and ISI-MIP as well as from the wheat and maize pilots of AgMIP suggest that the uncertainty from different impact models is typically larger than that from different climate scenarios (Asseng, et al., 2013, Rosenzweig, et al., 2013a). More work to analyze underlying reasons and to improve model projections is needed and will be coordinated by AgMIP. A harmonization of assumed management (growing periods, cultivars, fertilizers, pest control) will be central to understand differences in climate change impact assessments and will allow for separating impact uncertainty in uncertainty from management and uncertainty from climate impacts.

References

Ainsworth, E. A., Long, S. P., 2005. What have we learned from 15 years of free-air CO2 enrichment (FACE)? A meta-analytic review of the responses of photosynthesis, canopy properties and plant production to rising CO2, *New Phytologist.* **165**, 351-371.

Asseng, S., Ewert, F., Rosenzweig, C., Jones, J. W., Hatfield, J. L., Ruane, A. C., Boote, K. J., Thorburn, P. J., Rotter, R. P., Cammarano, D., Brisson, N., Basso, B., Martre, P., Aggarwal, P. K., Angulo, C., Bertuzzi, P., Biernath, C., Challinor, A. J., Doltra, J., Gayler, S., Goldberg, R., Grant, R., Heng, L., Hooker, J., Hunt, L. A., Ingwersen, J., Izaurralde, R. C., Kersebaum, K. C., Muller, C., Naresh Kumar, S., Nendel, C., O/'Leary, G., Olesen, J. E., Osborne, T. M., Palosuo, T., Priesack, E., Ripoche, D., Semenov, M. A., Shcherbak, I., Steduto, P., Stockle, C., Stratonovitch, P., Streck, T., Supit, I., Tao, F., Travasso, M., Waha, K., Wallach, D., White, J. W., Williams, J. R., Wolf, J., 2013. Uncertainty in simulating wheat yields under climate change, *Nature Clim. Change.* **advance online publication**.

Asseng, S., Foster, I., Turner, N. C., 2011. The impact of temperature variability on wheat yields, *Global Change Biology.* **17**, 997-1012.

Basso, B., Gargiulo, O., Paustian, K., Robertson, G. P., Porter, C., Grace, P. R., Jones, J. W., 2011. Procedures for Initializing Soil Organic Carbon Pools in the DSSAT-CENTURY Model for Agricultural Systems, *Soil Science Society of America Journal.* **75**, 69-78.

Bender, J., Weigel, H. J., 2011. Changes in atmospheric chemistry and crop health: A review, *Agronomy for Sustainable Development.* **31**, 81-89.

Berding, N., Hurney, A. P., 2005. Flowering and lodging, physiological-based traits affecting cane and sugar yield: What do we know of their control mechanisms and how do we manage them?, *Field Crops Research.* **92**, 261-275.

Bloom, A. J., Burger, M., Asensio, J. S. R., Cousins, A. B., 2010. Carbon Dioxide Enrichment Inhibits Nitrate Assimilation in Wheat and Arabidopsis, *Science.* **328**, 899-903.

Bondeau, A., Smith, P. C., Zaehle, S., Schaphoff, S., Lucht, W., Cramer, W., Gerten, D., Lotze-Campen, H., Müller, C., Reichstein, M., Smith, B., 2007. Modelling the role of agriculture for the 20th century global terrestrial carbon balance, *Global Change Biology.* **13**, 679-706.

Cai, X. M., Rosegrant, M. W., 2002. Global water demand and supply projections part - 1. A modeling approach, *Water International.* **27**, 159-169.

Capehart, T., Allen, E., Bond, J., 2012. Feed outlook: Increased Foreign Corn Production Finds Strong Demand.

Cosby, B. J., Hornberger, G. M., Clapp, R. B., Ginn, T. R., 1984. A Statistical Exploration of the Relationships of Soil-Moisture Characteristics to the Physical-Properties of Soils, *Water Resources Research.* **20**, 682-690.

Dermody, O., O'Neill, B. F., Zangerl, A. R., Berenbaum, M. R., DeLucia, E. H., 2008. Effects of elevated CO2 and O-3 on leaf damage and insect abundance in a soybean agroecosystem, *Arthropod-Plant Interact.* **2**, 125-135.

Dietrich, J. P., Schmitz, C., Lotze-Campen, H., Popp, A., Müller, C., in press. An outlook on agricultural productivity - Implementing endogenous technological change in a global land-use model, *Environmental & Resource Economics*.

Dietrich, J. P., Schmitz, C., Müller, C., Fader, M., Lotze-Campen, H., Popp, A., 2012. Measuring agricultural land-use intensity - A global analysis using a model-assisted approach, *Ecological Modelling.* **232**, 109-118.

Dufresne, J. L., Foujols, M. A., Denvil, S., Caubel, A., Marti, O., Aumont, O., Balkanski, Y., Bekki, S., Bellenger, H., Benshila, R., Bony, S., Bopp, L., Braconnot, P., Brockmann, P., Cadule, P., Cheruy, F., Codron, F., Cozic, A., Cugnet, D., Noblet, N., Duvel, J. P., Ethé, C., Fairhead, L., Fichefet, T., Flavoni, S., Friedlingstein, P., Grandpeix, J. Y., Guez, L., Guilyardi, E., Hauglustaine, D., Hourdin, F., Idelkadi, A., Ghattas, J., Joussaume, S., Kageyama, M., Krinner, G., Labetoulle, S., Lahellec, A., Lefebvre, M. P., Lefevre, F., Levy, C., Li, Z. X., Lloyd, J., Lott, F., Madec, G., Mancip, M., Marchand, M., Masson, S., Meurdesoif, Y., Mignot, J., Musat, I., Parouty, S., Polcher, J., Rio, C., Schulz, M., Swingedouw, D., Szopa, S., Talandier, C., Terray, P., Viovy, N., Vuichard, N., 2013. Climate change projections using the IPSL-CM5 Earth System Model: from CMIP3 to CMIP5, *Climate Dynamics.* **40**, 2123-2165.

Fader, M., Rost, S., Müller, C., Bondeau, A., Gerten, D., 2010. Virtual water content of temperate cereals and maize: Present and potential future patterns, *Journal of Hydrology.* **384**, 218-231.

FAO/IIASA/ISRIC/ISSCAS/JRC, 2012. Harmonized World Soil Database (version 1.2), FAO, Rome, Italy and IIASA, Laxenburg, Austria. available at http://www.iiasa.ac.at/Research/LUC/External-World-soil-database/HTML/.

Folberth, C., Gaiser, T., Abbaspour, K. C., Schulin, R., Yang, H., 2012. Regionalization of a large-scale crop growth model for sub-Saharan Africa: Model setup, evaluation, and estimation of maize yields, *Agric Ecosyst Environ.* **151**, 21-33.

Fujimori, S., Masui, T., Matsuoka, Y., 2012. AIM/CGE [basic] manual.

Geng, S., Auburn, J., Brandstetter, E., Li, B., 1988. A program to simulate meteorological variables: documentation for SIMMETEO.

Geng, S., Penning de Vries, F. W. T., Supit, I., 1986. A simple method for generating daily rainfall data, *Agricultural and Forest Meteorology.* **36**, 363-376.

Gosme, M., Suffert, F., Jeuffroy, M. H., 2010. Intensive versus low-input cropping systems: What is the optimal partitioning of agricultural area in order to reduce pesticide use while maintaining productivity?, *Agricultural Systems.* **103**, 110-116.

Havlík, P., Schneider, U. A., Schmid, E., Böttcher, H., Fritz, S., Skalský, R., Aoki, K., Cara, S. D., Kindermann, G., Kraxner, F., Leduc, S., McCallum, I., Mosnier, A., Sauer, T., Obersteiner, M., 2011. Global land-use implications of first and second generation biofuel targets, *Energy Policy.* **39**, 5690-5702.

Havlík, P., Valin, H., Mosnier, A., Obersteiner, M., Baker, J. S., Herrero, M., Rufino, M. C., Schmid, E., 2013. Crop Productivity and the Global Livestock Sector: Implications for Land Use Change and Greenhouse Gas Emissions, *American Journal of Agricultural Economics.* **95**, 442-448.

Hawkins, E., Fricker, T. E., Challinor, A. J., Ferro, C. A. T., Ho, C. K., Osborne, T. M., 2013. Increasing influence of heat stress on French maize yields from the 1960s to the 2030s, *Global Change Biology.* **in press**.

Hawkins, E., Sutton, R., 2009. The potential to narrow uncertainty in regional climate predictions, *Bulletin of the American Meteorological Society.* **90**, 1095-1107.

Hawkins, E., Sutton, R., 2011. The potential to narrow uncertainty in projections of regional precipitation change, *Climate Dynamics.* **37**, 407-418.

Haxeltine, A., Prentice, I. C., 1996. BIOME3: An equilibrium terrestrial biosphere model based on ecophysiological constraints, resource availability, and competition among plant functional types, *Global Biogeochemical Cycles.* **10**, 693-709.

Hempel, S., Frieler, K., Warszawski, L., Schewe, J., Piontek, F., 2013. A trend-preserving bias correction -- the ISI-MIP approach, *Earth System Dynamics Discussions.* **4**, 49-92.

Hoogenboom, G., Jones, J. W., Wilkens, P. W., Porter, C. H., Batchelor, W. D., Hunt, L. A., Boote, K. J., Singh, U., Uryasev, O., Bowen, W. T., Gijsman, A. J., Toit, A. S. D., White, J. W., Tsuji, G. Y., 2004. Decision Support System for Agrotechnology Transfer Version 4.0 [CD-ROM].

Jobbágy, E. G., Jackson, R. B., 2000. THE VERTICAL DISTRIBUTION OF SOIL ORGANIC CARBON AND ITS RELATION TO CLIMATE AND VEGETATION, *Ecological Applications.* **10**, 423-436.
Jones, C. D., Hughes, J. K., Bellouin, N., Hardiman, S. C., Jones, G. S., Knight, J., Liddicoat, S., O'Connor, F. M., Andres, R. J., Bell, C., Boo, K. O., Bozzo, A., Butchart, N., Cadule, P., Corbin, K. D., Doutriaux-Boucher, M., Friedlingstein, P., Gornall, J., Gray, L., Halloran, P. R., Hurtt, G., Ingram, W. J., Lamarque, J. F., Law, R. M., Meinshausen, M., Osprey, S., Palin, E. J., Parsons Chini, L., Raddatz, T., Sanderson, M. G., Sellar, A. A., Schurer, A., Valdes, P., Wood, N., Woodward, S., Yoshioka, M., Zerroukat, M., 2011. The HadGEM2-ES implementation of CMIP5 centennial simulations, *Geosci. Model Dev.* **4**, 543-570.
Jones, J. W., Hoogenboom, G., Porter, C. H., Boote, K. J., Batchelor, W. D., Hunt, L. A., Wilkens, P. W., Singh, U., Gijsman, A. J., Ritchie, J. T., 2003. The DSSAT cropping system model, *European Journal of Agronomy.* **18**, 235-265.
Knox, J., Hess, T., Daccache, A., Wheeler, T., 2012. Climate change impacts on crop productivity in Africa and South Asia, *Environmental Research Letters.* **7**, 034032.
Koo, J., Dimes, J., 2010. HC27 Generic Soil Profile Database, Version 1, International Food Policy Research Institute. available at http://hdl.handle.net/1902.1/20299.
Lapola, D. M., Priess, J. A., Bondeau, A., 2009. Modeling the land requirements and potential productivity of sugarcane and jatropha in Brazil and India using the LPJmL dynamic global vegetation model, *Biomass and Bioenergy.* **33**, 1087-1095.
Laux, P., Jacket, G., Tingem, R. M., Kunstmann, H., 2010. Impact of climate change on agricultural productivity under rainfed conditions in Cameroon-A method to improve attainable crop yields by planting date adaptations, *Agricultural and Forest Meteorology.* **150**, 1258-1271.
Lawrence, D. M., Slater, A. G., 2008. Incorporating organic soil into a global climate model, *Climate Dynamics.* **30**, 145-160.
Leakey, A. D. B., Ainsworth, E. A., Bernacchi, C. J., Rogers, A., Long, S. P., Ort, D. R., 2009. Elevated CO2 effects on plant carbon, nitrogen, and water relations: six important lessons from FACE, *Journal of Experimental Botany.* **60**, 2859-2876.
Leisner, C. P., Ainsworth, E. A., 2012. Quantifying the effects of ozone on plant reproductive growth and development, *Global Change Biology.* **18**, 606-616.
Lobell, D. B., Banziger, M., Magorokosho, C., Vivek, B., 2011. Nonlinear heat effects on African maize as evidenced by historical yield trials, *Nature Climate Change.* **1**, 42-45.
Long, S. P., Ainsworth, E. A., Leakey, A. D. B., Nosberger, J., Ort, D. R., 2006. Food for Thought: Lower-Than-Expected Crop Yield Stimulation with Rising CO2 Concentrations, *Science.* **312**, 1918-1921.
Lotze-Campen, H., Müller, C., Bondeau, A., Rost, S., Popp, A., Lucht, W., 2008. Global food demand, productivity growth and the scarcity of land and water resources: a spatially explicit mathematical programming approach, *Agric. Econ.* **39**, 325-338
Moss, R. H., Edmonds, J. A., Hibbard, K. A., Manning, M. R., Rose, S. K., van Vuuren, D. P., Carter, T. R., Emori, S., Kainuma, M., Kram, T., Meehl, G. A., Mitchell, J. F. B., Nakicenovic, N., Riahi, K., Smith, S. J., Stouffer, R. J., Thomson, A. M., Weyant, J. P., Wilbanks, T. J., 2010. The next generation of scenarios for climate change research and assessment, *Nature.* **463**, 747-756.
Müller, C., 2011. Harvesting from Uncertainties, *Nature Climate Change.* **1**, 253-254.
Müller, C., Cramer, W., Hare, W. L., Lotze-Campen, H., 2011. Climate change risks for African agriculture, *Proceedings of the National Academy of Sciences of the United States of America.* **108**, 4313-4315.
Müller, C., Waha, K., Bondeau, A., Heinke, J., 2013. Hotspots and implications of climate change impacts in sub-Saharan Africa, *Nature Climate Change.* **submitted**.

Nelson, G. C., Mensbrugghe, D. v. d., Blanc, E., Calvin, K., Hasegawa, T., Havlík, P., Kyle, P., Lotze-Campen, H., Lampe, M. v., d'Croz, D. M., Meijl, H. v., Müller, C., Reilly, J., Robertson, R., Sands, R. D., Schmitz, C., Tabeau, A., Takahashi, K., Valin, H., 2013. Agriculture and Climate Change in Global Scenarios: Why Don't the Models Agree, *Agric. Econ.* **this issue**.

Nelson, G. C., Rosegrant, M. W., Palazzo, A., Gray, I., Ingersoll, C., Robertson, R., Tokgoz, S., Zhu, T., Sulser, T. B., Ringler, C., Msangi, S., You, L., 2010. *Food Security, Farming, and Climate Change to 2050*. International Food Policy Research Institute, Washington, D.C., USA.

Paltsev, S., Reilly, J. M., Jacoby, H. D., Eckaus, R. S., McFarland, J., Sarofim, M., Asadoorian, M., Babiker, M., 2005. The MIT Emissions Prediction and Policy Analysis (EPPA) Model: Version 4, available at http://globalchange.mit.edu/research/publications/697.

Parry, M. A. J., Hawkesford, M. J., 2010. Food security: increasing yield and improving resource use efficiency, *Proc Nutr Soc.* **69**, 592-600.

Piani, C., Haerter, J. O., Coppola, E., 2010. Statistical bias correction for daily precipitation in regional climate models over Europe, *Theoretical and Applied Climatology.* **99**, 187-192.

Portmann, F. T., Siebert, S., Döll, P., 2010. MIRCA2000-Global monthly irrigated and rainfed crop areas around the year 2000: A new high-resolution data set for agricultural and hydrological modeling, *Global Biogeochemical Cycles.* **24**, Gb1011.

Prince, S. D., Haskett, J., Steininger, M., Strand, H., Wright, R., 2001. Net Primary Production of U.S. Midwest Croplands from Agricultural Harvest Yield Data, *Ecological Applications.* **11**, 1194-1205.

Randall, D. A., Wood, R. A., Bony, S., Colman, R., Fichefet, T., Fyfe, J., Kattsov, V., Pitman, A., Shukla, J., Srinivasan, J., Stouffer, R. J., Sumi, A., Taylor, K. E., 2007. Cilmate Models and Their Evaluation, in S. Solomon, D. Qin, M. Manning, Z. Chen, M. Marquis, K. B. Averyt, M.Tignor and H. L. Miller eds., *Climate Change 2007: The Physical Science Basis. Contribution of Working Group I to the Fourth Assessment Report of the Intergovernmental Panel on Climate Change* Cambridge University Press, Cambridge, United Kingdom and New York, NY, USA.

Rawls, W. J., Brakensiek, D. L., Miller, N., 1983. Green-Ampt Infiltration Parameters from Soils Data, *Journal of Hydraulic Engineering-Asce.* **109**, 62-70.

Riahi, K., Rao, S., Krey, V., Cho, C., Chirkov, V., Fischer, G., Kindermann, G., Nakicenovic, N., Rafaj, P., 2011. RCP 8.5—A scenario of comparatively high greenhouse gas emissions, *Climatic Change.* **109**, 33-57.

Ribeiro, D. M., Araújo, W. L., Fernie, A. R., Schippers, J. H. M., Mueller-Roeber, B., 2012. Action of Gibberellins on Growth and Metabolism of Arabidopsis Plants Associated with High Concentration of Carbon Dioxide.

Rosegrant, M. W., IMPACT Development Team, 2012. International Model for Policy Analysis of Agricultural Commodities and Trade (IMPACT) Model Description, available at http://www.ifpri.org/publication/international-model-policy-analysis-agricultural-commodities-and-trade-impact-1.

Rosenzweig, C., Elliott, J., Deryng, D., Ruane, A. C., Arneth, A., Boote, K. J., Folberth, C., Glotter, M., Khabarov, N., Müller, C., Neumann, K., Piontek, F., Pugh, T. A. M., Schmid, E., Stehfest, E., Jones, J. W., 2013a. Assessing agricultural risks of climate change in the 21st century in a global gridded crop model intercomparison, *Proceedings of the National Academy of Sciences of the United States of America.* **in press**.

Rosenzweig, C., Jones, J. W., Hatfield, J. L., Ruane, A. C., Boote, K. J., Thorburne, P., Antle, J. M., Nelson, G. C., Porter, C., Janssen, S., Asseng, S., Basso, B., Ewert, F., Wallach, D., Baigorria, G., Winter, J. M., 2013b. The Agricultural Model Intercomparison and Improvement Project (AgMIP): Protocols and pilot studies, *Agricultural and Forest Meteorology.* **170**, 166-182.

Rötter, R. P., Carter, T. R., Olesen, J. E., Porter, J. R., 2011. Crop-climate models need an overhaul, *Nature Clim. Change.* **1**, 175-177.

Roudier, P., Sultan, B., Quirion, P., Berg, A., 2011. The impact of future climate change on West African crop yields: What does the recent literature say?, *Global Environmental Change.* **21**, 1073-1083.

Schaphoff, S., Heyder, U., Ostberg, S., Gerten, D., Heinke, J., Lucht, W., 2013. Contribution of permafrost soils to the global carbon budget, *Environmental Research Letters.* **8**, 014026.

Schmitz, C., Biewald, A., Lotze-Campen, H., Popp, A., Dietrich, J. P., Bodirsky, B., Krause, M., Weindl, I., 2012. Trading more food: Implications for land use, greenhouse gas emissions, and the food system, *Global Environmental Change.* **22**, 189-209.

Schmitz, C., Lotze-Campen, H., Popp, A., Krause, M., Dietrich, J. P., Müller, C., 2013. Agricultural trade and tropical deforestation - Interactions and related policy options, *Reg. Envir. Chang.* **under review**.

Singels, A., Donaldson, R. A., Smit, M. A., 2005. Improving biomass production and partitioning in sugarcane: theory and practice, *Field Crops Research.* **92**, 291-303.

Taylor, K. E., Stouffer, R. J., Meehl, G. A., 2012. An Overview of CMIP5 and the Experiment Design, *Bulletin of the American Meteorological Society.* **93**, 485-498.

Thomson, A., Calvin, K., Smith, S., Kyle, G., Volke, A., Patel, P., Delgado-Arias, S., Bond-Lamberty, B., Wise, M., Clarke, L., Edmonds, J., 2011. RCP4.5: a pathway for stabilization of radiative forcing by 2100, *Climatic Change.* **109**, 77-94.

Tubiello, F. N., Amthor, J. S., Boote, K. J., Donatelli, M., Easterling, W., Fischer, G., Gifford, R. M., Howden, M., Reilly, J., Rosenzweig, C., 2007. Crop response to elevated CO2 and world food supply - A comment on "Food for Thought..." by Long et al., Science 312 : 1918-1921, 2006, *European Journal of Agronomy.* **26**, 215-223.

von Lampe, M., Willenbockel, D., Blanc, E., Cai, Y., Calvin, K., Fujimori, S., Hasegawa, T., Havlík, P., Kyle, P., Lotze-Campen, H., d'Croz, D. M., Nelson, G. D., Sands, R. D., Schmitz, C., Tabeau, A., Valin, H., Mensbrugghe, D. v. d., Meijl, H. v., 2013. Why Do Global Long-term Scenarios for Agriculture Differ? An overview of the AgMIP Global Economic Model Intercomparison, *Agric. Econ.* **this issue**.

Waha, K., Müller, C., Bondeau, A., Dietrich, J., Kurukulasuriya, P., Heinke, J., Lotze-Campen, H., 2013. Adaptation to climate change through the choice of cropping system and sowing date in sub-Saharan Africa, *Global Environmental Change.* **23**, 130-143.

Waha, K., van Bussel, L. G. J., Müller, C., Bondeau, A., 2012. Climate-driven simulation of global crop sowing dates, *Global Ecology and Biogeography.* **21**, 247-259.

Weedon, G. P., Gomes, S., Viterbo, P., Shuttleworth, W. J., Blyth, E., Österle, H., Adam, J. C., Bellouin, N., Boucher, O., Best, M., 2011. Creation of the WATCH Forcing Data and Its Use to Assess Global and Regional Reference Crop Evaporation over Land during the Twentieth Century, *Journal of Hydrometeorology.* **12**, 823-848.

Wild, O., Fiore, A. M., Shindell, D. T., Doherty, R. M., Collins, W. J., Dentener, F. J., Schultz, M. G., Gong, S., MacKenzie, I. A., Zeng, G., Hess, P., Duncan, B. N., Bergmann, D. J., Szopa, S., Jonson, J. E., Keating, T. J., Zuber, A., 2012. Modelling future changes in surface ozone: a parameterized approach, *Atmospheric Chemistry and Physics.* **12**, 2037-2054.

Wise, M., Calvin, K., 2011. GCAM 3.0 Agriculture and Land Use: Technical Description of Modeling Approach, available at https://wiki.umd.edu/gcam/images/8/87/GCAM3AGTechDescript12_5_11.pdf.

You, L., S.Crespo, Guo, Z., Koo, J., Ojo, W., Sebastian, K., Tenorio, M. T., Wood, S., ., U. W.-S., 2010. Spatial Produciton Allocation Model (SPAM) 2000 Version 3 Release 2, available at http://MapSPAM.info.

Zavala, J. A., Casteel, C. L., DeLucia, E. H., Berenbaum, M. R., 2008. Anthropogenic increase in carbon dioxide compromises plant defense against invasive insects, *Proceedings of the National Academy of Sciences of the United States of America.* **105**, 5129-5133.
Zhou, X., Zhu, Q., Tang, S., Chen, X., Wu, M., 2002. Interception of PAR and relationship between FPAR and LAI in summer maize canopy, *Geoscience and Remote Sensing Symposium IGARSS '02*.

Tables

Table 1: Mapping of biophysical crop yield simulations to agricultural economic commodities.

Agricultural economic commodity	**Mapping for DSSAT**	**Mapping for LPJmL**
Cassava	represented by the average climate effects on the 4 major C_3 crops modeled (**rice, wheat, soybeans, groundnuts**)	**Cassava** yield simulations directly applied
Groundnuts	**Groundnut** yield simulations directly applied	**Groundnut** yield simulations directly applied
Maize	**Maize** yield simulations directly applied	**Maize** yield simulations directly applied
Millet	represented by modified **maize** yield simulations, applying all the positive climate effects but only 50% of the negative effects due to better drought tolerance	**Millet** yield simulations directly applied
Rapeseed	represented by the average climate effects on the 4 major C_3 crops modeled (**rice, wheat, soybeans, groundnuts**)	**Rapeseed** yield simulations directly applied
Rice	**Rice** yield simulations directly applied	**Rice** yield simulations directly applied
Soybeans	**Soybean** yield simulations directly applied	**Soybean** yield simulations directly applied
Sugarcane	**Maize** yield simulations represent climate impacts on sugarcane	**Sugarcane** yield simulations directly applied
Sugar beet	represented by the average climate effects on the 4 major C_3 crops modeled (**rice, wheat, soybeans, groundnuts**)	**Sugar beet** yield simulations directly applied
Wheat	**Wheat** yield simulations directly applied	**Wheat** yield simulations directly

		applied
Sorghum	represented by modified **maize** yield simulations, applying all the positive climate effects but only 50% of the negative effects due to better drought tolerance	**Millet** yield simulations represent climate impacts on sorghum
Oilseeds (sunflower, palm, total other oilseeds)	represented by the average climate effects on the 4 major C_3 crops modeled (**rice, wheat, soybeans, groundnuts**)	Represented by **sunflower** yield simulations
Other Grains	represented by modified **wheat** yield simulations, applying all the positive climate effects but only 50% of the negative effects due to better drought tolerance	represented by modified **wheat** yield simulations, applying all the positive climate effects but only 50% of the negative effects due to better drought tolerance
Dryland Legumes (Chickpeas and Pigeon Peas)	represented by modified **groundnut** yield simulations, applying all the positive climate effects but only 50% of the negative effects due to better drought tolerance	represented by modified **groundnut** yield simulations, applying all the positive climate effects but only 50% of the negative effects due to better drought tolerance
Other C_3 crops (cotton, potatoes, sweet potatoes and yams, subtropical fruit, temperate fruits, and vegetables)	represented by the average climate effects on the 4 major C_3 crops modeled (**rice, wheat, soybeans, groundnuts**)	represented by the average climate effects on the 4 major C_3 crops modeled (**rice, wheat, soybeans, groundnuts**)

Table 2: projected changes in global productivity in percent for the five crops simulated by both models; wheat, maize, rice, soybean and groundnut

	Hadley		IPSL	
	DSSAT	LPJmL	DSSAT	LPJmL
wheat	-17.7%	-11.5%	-21.0%	-12.9%
maize	-37.6%	-9.9%	-33.9%	-14.2%
rice	-15.7%	-18.2%	-16.4%	-16.1%
soybean	-16.8%	-20.%	-13.0%	-29.8%
groundnut	-20.9%	-24.3%	-18.4%	-21.2%

Figures

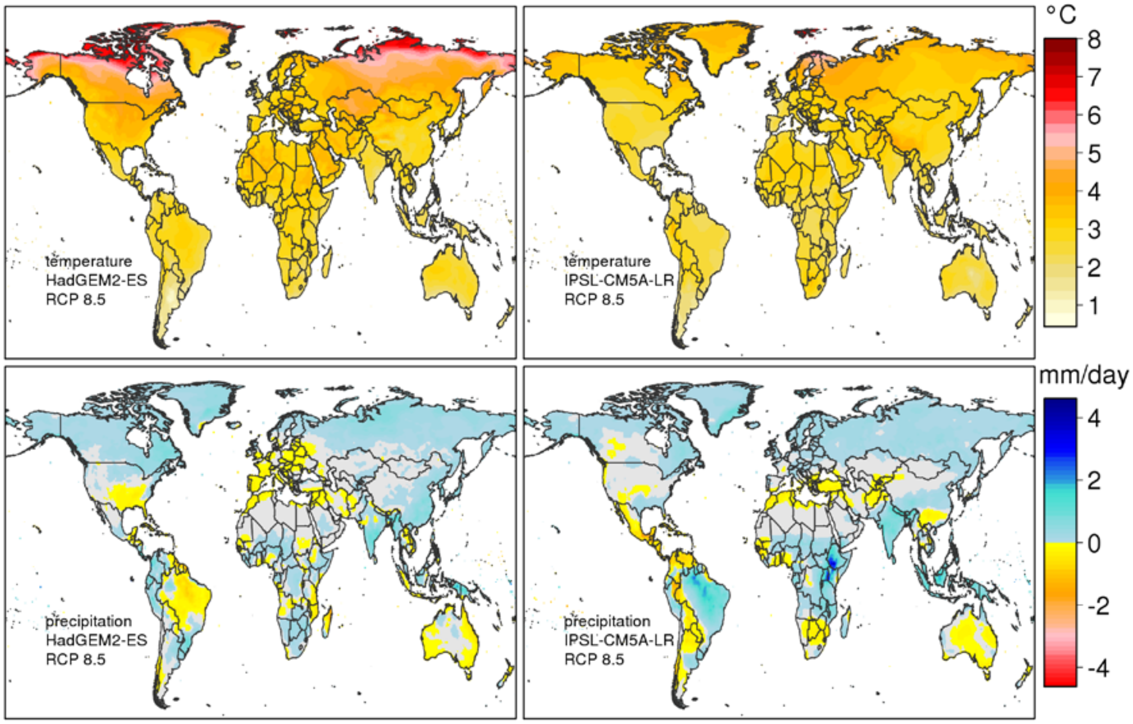

Figure 1: Absolute changes in annual mean temperature [°C] (top) and annual mean precipitation [mm/day] (bottom) from 1980-2010 to 2035-2065 for the HadGEM-ES2 (left) and IPSL-CM5A-LR (right) models. Temperature changes above 8°C have been cut to facilitate better visibility of differences at lower temperature changes, which is more important for cultivated areas. Grey areas in the bottom depict regions with precipitation changes of less than 50mm/year (0.137mm/day). Seasonal changes are depicted in the supplementary Figures S1-S4.

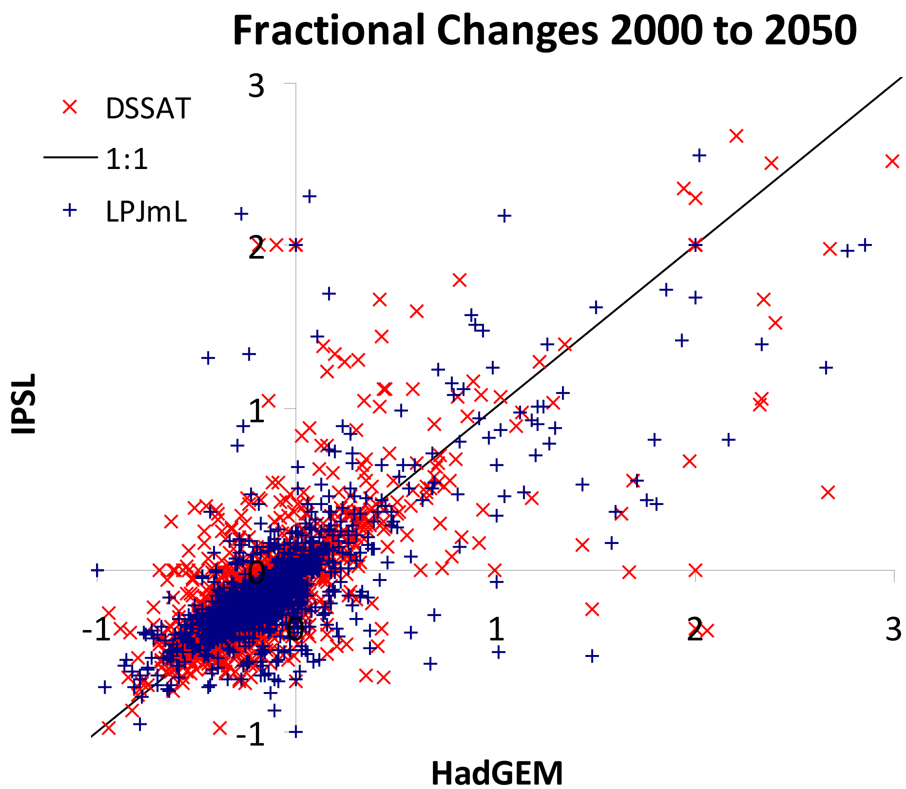

Figure 2: Fractional changes (P_{fut}/P_{ref})-1 in crop productivity comparing the 2 crop models (red x: DSSAT, blue +: LPJmL) and climate models HadGEM (x-axis) and IPSL (y-axis) for the 5 jointly simulated crops (maize, wheat, rice, soybean, groundnut) for all FPUs.

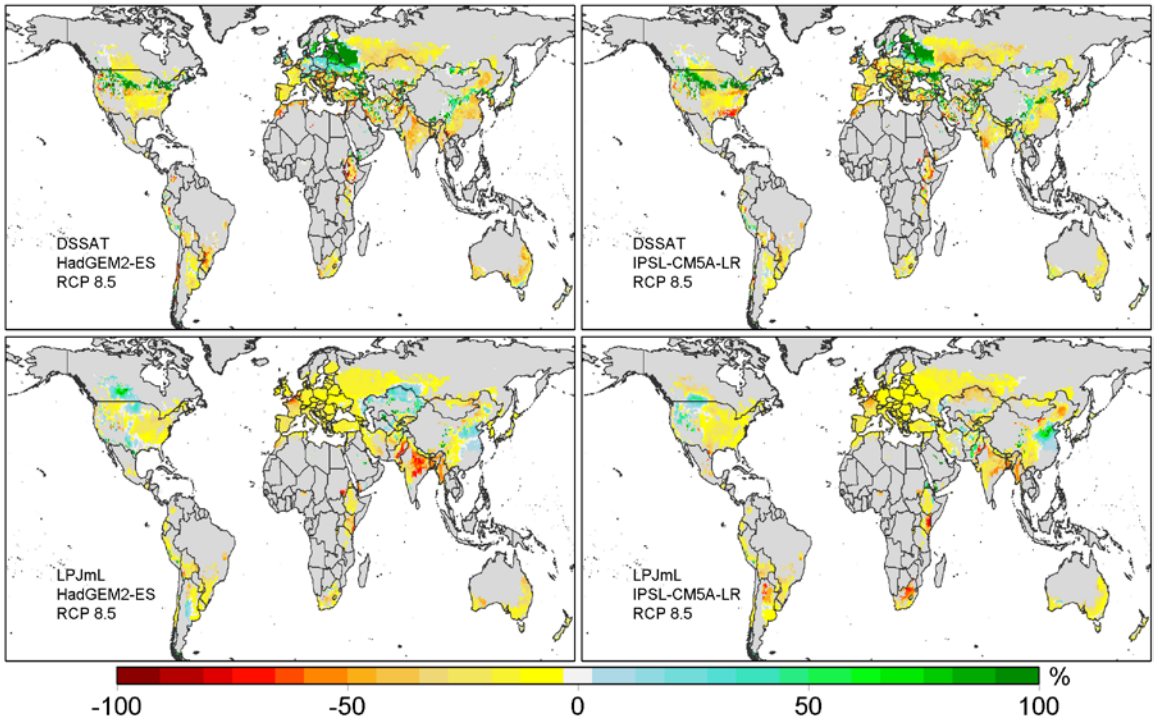

Figure 3: Relative changes in rainfed wheat productivity as projected by DSSAT (top) and LPJmL (bottom) for the HadGEM-ES2 (left) and IPSL-CM5A-LR (right) climate scenarios for the RCP8.5 emission scenario. Dark grey areas are currently not used for cultivation of rainfed wheat (Portmann, et al., 2010).

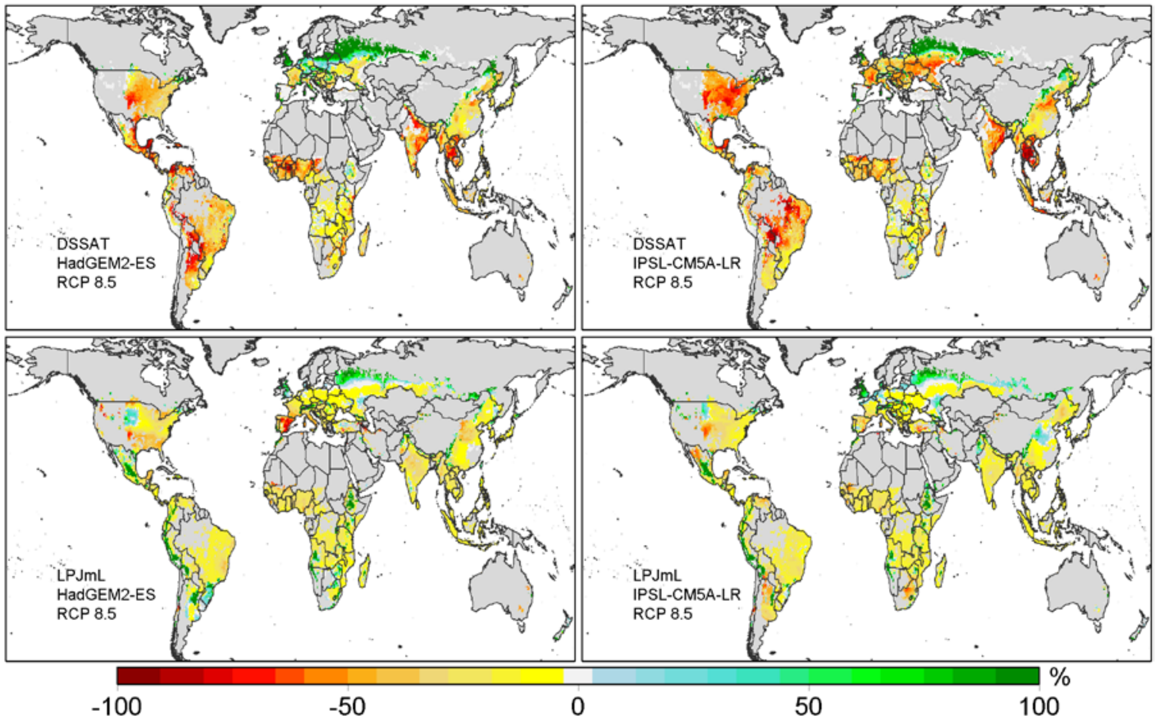

Figure 4: Relative changes in rainfed maize productivity as projected by DSSAT (top) and LPJmL (bottom) for the HadGEM-ES2 (left) and IPSL-CM5A-LR (right) climate scenarios for the RCP8.5 emission scenario. Dark grey areas are currently not used for cultivation of rainfed maize (Portmann, et al., 2010).

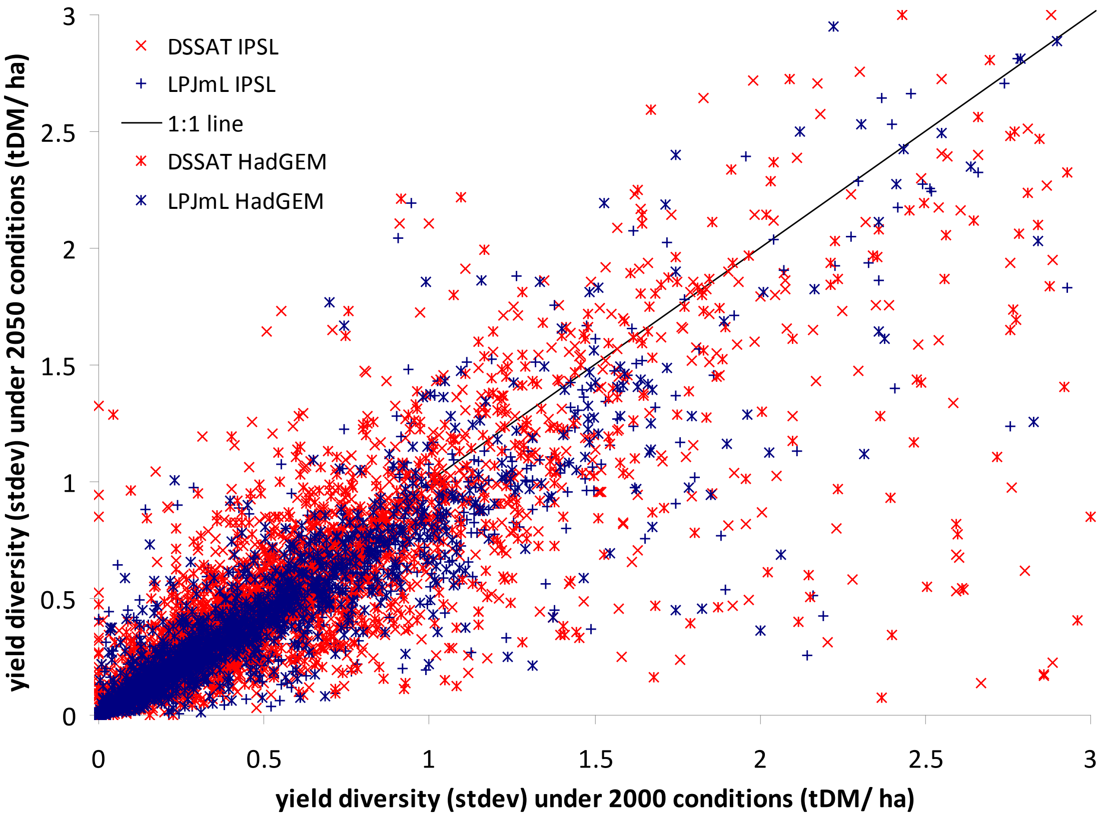

Figure 5: Yield diversity in food production units (FPU, i.e. across pixels within a FPU) decreases more often than increases under climate change. Blue symbols indicate yield diversity as simulated with LPJmL, red symbols indicate yield diversity as simulated by DSSAT. Crosses (×) indicate simulations for IPSL-CM5A-LR climate scenario, double-crosses (∗) indicate simulations for HadGEM2-ES.

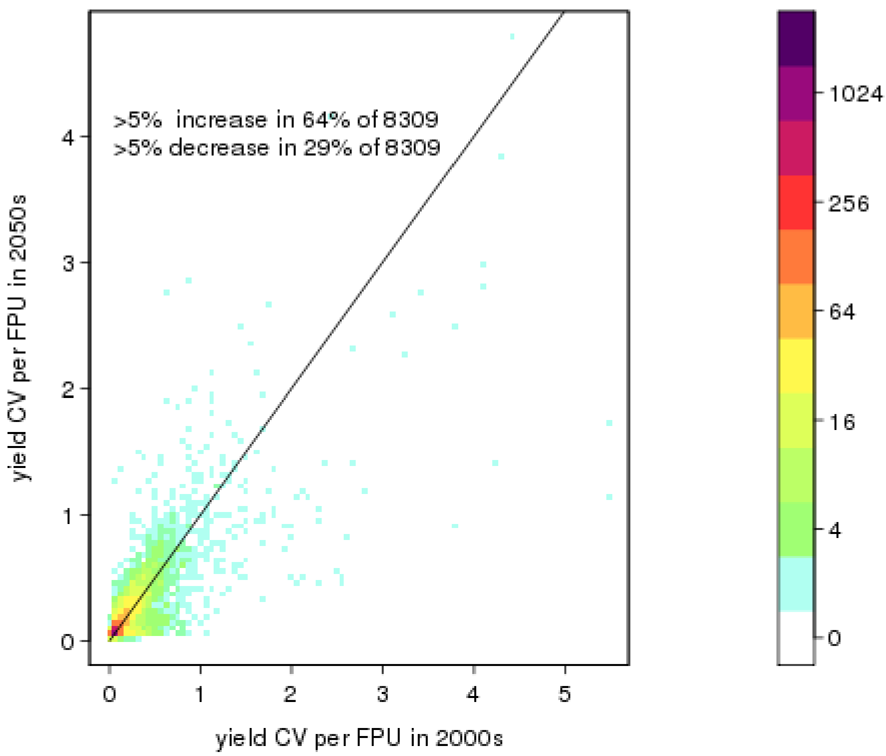

Figure 6: Year-to-year variability increases more often than decreases. Colors depict point density in the scatter plot (log scale). The total number of FPUs (8309) is the sum of FPUs (max 281) for the 12 LPJmL crops simulated here summed for irrigated and rainfed management systems and for 2 climate scenarios. Black line is 1:1 line.